Microlenses for astrophotonic instruments manufactured by ultrafast-laser assisted etching

Proceedings Volume 11451, Advances in Optical and Mechanical Technologies for Telescopes and Instrumentation IV; 114510P (2020) https://doi.org/10.1117/12.2561481

PROCEEDINGS OF SPIE

SPIEDigitalLibrary.org/conference-proceedings-of-spie

Microlenses for astrophotonic instruments manufactured by ultrafast-laser assisted etching

Ross, Calum, Lee, David, Guinouard, Isabelle, Thomson, Robert

Calum A. Ross, David Lee, Isabelle Guinouard, Robert R. Thomson, "Microlenses for astrophotonic instruments manufactured by ultrafast-laser assisted etching," Proc. SPIE 11451, Advances in Optical and Mechanical Technologies for Telescopes and Instrumentation IV, 114510P (13 December 2020); doi: 10.1117/12.2561481

SPIE.

Event: SPIE Astronomical Telescopes + Instrumentation, 2020, Online Only

Microlenses for astrophotonic instruments manufactured by ultrafast-laser assisted etching

Calum A. Ross*[a], David Lee[b], Isabelle Guinouard[c], Robert R. Thomson[a]
[a]Institute of Photonics and Quantum Sciences, Heriot-Watt University Edinburgh, EH14 4AS, U.K.; [b]Science and Technology Facilities Council, UK Astronomy Technology Centre, Royal Observatory, Blackford Hill, Edinburgh, EH9 3HJ, U.K.; [c]GEPI, Observatoire de Paris, PSL Research University, CNRS, 5 Place Jules Janssen 92195, Meudon, France

ABSTRACT

The performance of astrophotonic instruments is determined by various factors including the quality of optical surfaces and the precise alignment of components. As instruments become more complex and compact, the manufacture and assembly of components is increasingly challenging. We propose that a laser-based glass microfabrication technique known as ultrafast-laser assisted etching (ULAE) is ideally suited to the manufacture of both existing and novel components for astrophotonic instruments. To demonstrate this potential, we will present ULAE manufactured micro-lenses with integrated passive alignment features for efficient optical fiber coupling. A full physical and optical characterization of the micro-lenses is given. These components have applications in fiber-fed multi-object spectrographs.

Keywords: microlens; direct laser writing; fused silica; passive alignment; multi-object spectroscopy; ultrafast laser assisted etching

1. INTRODUCTION

As photonic technologies progress, astrophotonic instrumentation is becoming ever more complex with a drive to fully utilize the potential of extremely large telescopes. An example of such an instrument is the Multi-Object Optical and Near-infrared Spectrograph (MOONS)[1]. MOONS is a multi-object near-infrared spectrograph under construction for the Very Large Telescope (VLT), Paranal Observatory, Chile. MOONS employs an optical fiber positioning system which allows for independent positioning of 1000 fibers at the instrument focal plane for coupling starlight to two spectrographs for analysis[2]. The vast quantity of fibers and accompanying electronics, mechanics and optics presented a tremendous challenge for the researchers. Such systems are often costly, difficult to assemble and limited by manufacturability constraints[3]. Therefore, there is a need to explore methods of manufacturing which can overcome some of these limitations.

Methods of fabricating miniaturized optical components include precision diamond turning, lithography, and micro-molding. These techniques are enabling for a vast number of applications; however, each also has key limitations. Diamond turning offers high repeatability and precision of single element micro-optics with relatively simple surface forms but is less suitable for complex profiles. Lithography techniques are well established for the semiconductor industry and are therefore robust and highly cost-effective; however, these techniques are inherently planar and so unsuitable for manufacturing larger optical systems. Micro-molding permits greatest form freedom but is limited to low temperature glasses and polymers and requires expensive molds to be machined first. Consequently, these techniques are unsuitable for fabricating certain bespoke multi-element micro-optic components in a high-quality material such as fused silica.

An alternative technique that has the potential to fulfil this microfabrication niche is femtosecond laser writing followed by selective chemical etching. This technique, sometimes shortened to ultrafast laser assisted etching (ULAE), is a two-step three-dimensional (3D) subtractive manufacturing process compatible with fused silica glass. In the first step, ultrashort laser pulses (typically < 1 ps) are focused into a transparent (i.e. bandgap > photon energy) dielectric substrate. The high peak intensity associated with the ultrashort pulses induces nonlinear multiphoton absorption, and subsequent ionization, locally withing the focus. Meanwhile, the surrounding material is unaffected. Depending on the irradiation conditions, several permanent material modifications can be induced, each resulting from a change to the materials local molecular structure. The modification may include a change (typically an increase) to the refractive index of the inscribed material, or an increase in the materials susceptibility to chemical etching. The former modification has been used extensively for manufacturing integrated photonic waveguide devices such as photonic lanterns[4], gratings[5,6] and couplers[7]

Advances in Optical and Mechanical Technologies for Telescopes and Instrumentation IV,
edited by Ramón Navarro, Roland Geyl, Proc. of SPIE Vol. 11451, 114510P
© 2020 SPIE · CCC code: 0277-786X/20/$21 · doi: 10.1117/12.2561481

amongst others. The etching enhancement enables near arbitrarily shaped fused silica structures to be fabricated, with a feature resolution on the order of a few microns and a maximum component size limited only by the working distance of the objective lens that focuses pulses into the substrate, and the translation limits of the substrate with respect to the focus. The technique offers several desirable qualities including high-level automation, rapid prototyping and low feasibility cost. Additionally, due to the 3D nature of the laser writing process, ULAE permits freeform surface fabrication and does not suffer from *undercutting* which often limits the design freedom for molded parts. Further still, ULAE allows several components to be laser-written and etched on a single substrate, with each component passively aligned to the next with a precision set by the translation of the substrate – typically tens of nanometers for modern translation stages. This technique has been studied widely in literature and used to fabricate micro-optics[8], microfluidics[9] and lab-on-chip devices[10].

In this paper, we explore the potential of ULAE for fabricating optical components for fiber-based applications such as those found in fiber-fed multi-object spectrographs. More specifically, we fabricate fiber-coupled single lens collimators, originally specified for the MOONS instrument[11], with additional passive alignment features, and investigate some of the nuances associated with the fabrication process.

2. FABRICATION OF MICRO-COMPONENTS

2.1 Ultrafast laser inscription

Laser inscription was performed using a 350 fs fiber laser (BlueCut, Menlo Systems) delivering 1030 nm pulses at a repetition rate of 250 kHz. The laser beam was passed through a motorized zero-order half waveplate, polarizing beam splitter and second half waveplate to allow control of the pulse energy and linear polarization orientation. It is well known in the field that the etching rate after laser inscription is significantly enhanced if the polarization of the laser beam is aligned perpendicular to the substrate translation direction during laser writing[12]. This is due directional planes of birefringent material called *nanogratings* that form within the laser focus under certain irradiation parameters[13,14]. Therefore, the polarization orientation was set approximately perpendicular to the writing direction for the work presented here. For the curved lens surface, the polarization was aligned along the *y* axis. Two pulse energy regimes were investigated: 200 nJ and 600 nJ. The laser was focused into the substrate with a singlet aspheric lens with a numerical aperture of 0.3 to a diffraction limited spot with a theoretical beam waist of 2.2 μm and a confocal parameter of 10.6 μm in fused silica. The substrate was translated through the focus using a 3-axis, pneumatically counterbalanced crossed-roller-bearing translation stage (Alio Industries, AI-CM-2500) providing 100 nm translation precision, which was controlled with ACS Motion Control EtherCat controllers.

Components were inscribed in fused silica substrates (Corning HPSF 7980 0F grade) of 1 mm thickness in a "transverse" geometry, whereby the optical axis of the inscribed microlens lay orthogonally to the incident inscription beam. A schematic of the microlens, originally specified for the MOONS instrument[11], and accompanying fiber alignment slot is presented in Figure 1. A transverse writing geometry is favored in this case because the extent of the component along Z (the pointing direction of the inscription beam) is minimized and consequently, so are the depth dependent aberrations in the laser focus[15].

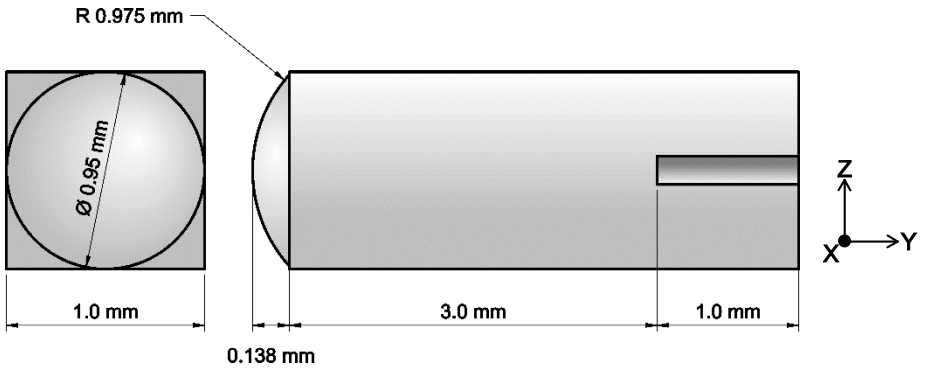

Figure 1: Schematic of the design specification for the MOONS lenses and the lenses fabricated in this work.

The micro-component was laser written by raster scanning the substrate through the laser focus to form each surface constructing the part. The surfaces were built up using a *bottom-up* approach to avoid laser writing through already

inscribed material. The surfaces were written at 1 mms^{-1} and the raster scan spacing was 2 µm. Inscribing a non-spherical lens surface, such as an aspheric or *best form* lens, is trivial using the direct laser writing approach. However, in order to allow for ease of characterization and comparison with commercially available spherical microlenses, the lens fabricated here was also spherical. The lens' clear aperture and focal length were designed to be 0.95 mm and the 3.0 mm respectively, giving an NA of approximately 0.23. A cylindrical slot, 1 mm in length, was inscribed into the substrate terminating at the focal point of the lens, for passive alignment of an optical fiber. The slot was designed to accommodate standard stripped 125 µm cladding diameter silica fiber but could be designed to accommodate any fiber such as the MOONS multimode fiber used to interface with the spectrograph[16].

2.2 Selective chemical etching

Following laser inscription, the substrate was submerged in an etching solution consisting of 8 mol L^{-1} potassium hydroxide (KOH) heated to 85˚C. These conditions have been reported to deliver an etching selectivity of up to 1000[17], whereby inscribed material dissolves 1000 times faster than the pristine glass when submerged in the etchant. The substrate was etched for approximately four hours, by which time the micro-optic had separated from the bulk substrate and the fiber alignment slot had fully formed. Micrographs of the fabricated micro-optic are presented in Figure 2.

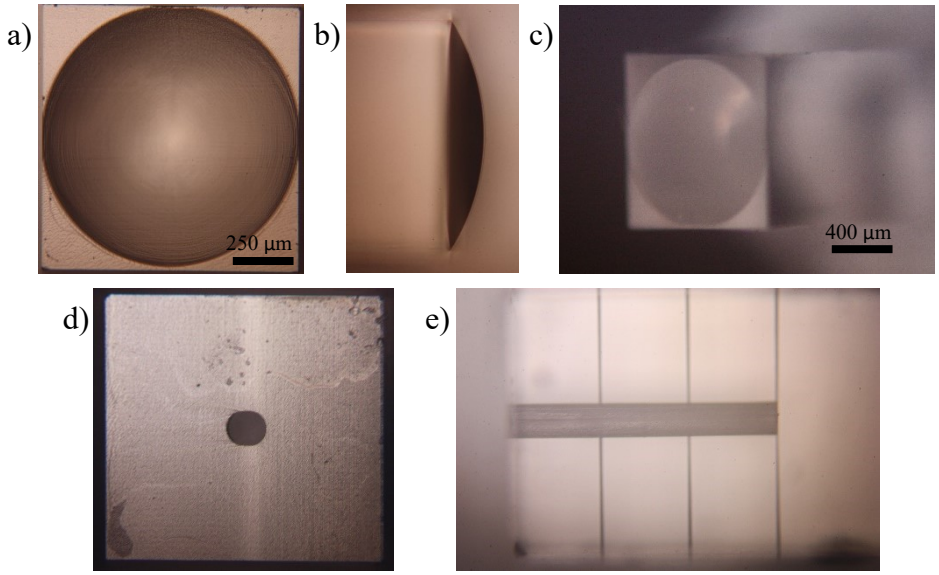

Figure 2: Micrographs of the fabricated micro-optic: the lens front view (a), side view (b) and isometric view (c), and the alignment slot end-on (d) and from the side (e) with additional channels to aid etching in view.

3. MICRO-OPTIC CHARACTERISATION AND PERFORMANCE

In this section, a characterization of the fiber coupler is presented. This includes: a physical lens surface characterization in terms of nominal form, surface texturing and roughness and a subsequent study of post process flame brushing to reduce roughness; a quantification of the passive alignment tolerance achieved by the fiber alignment slot; and an optical characterization in terms of throughput and fiber coupling efficiency.

3.1 Surface form

During the etching step, material is typically removed from the substrate from the outside inwards. This means that each surface, including the lens surface, experiences an etching gradient in terms of time spent in contact with etching solution. This results in an undesirable deviation from the inscribed surface form. This compensation can only be partially compensated for during the inscription stage due to unpredictable fluctuations in the etching process, and so achieving a high etching selectivity is a more robust approach. It is also worth noting that the laser affected zone within the focal volume is elliptical, and so the inscribed surface is not an exact replication of the toolpath, but rather a convolution of the toolpath and the modification volume. For simplicity, the toolpath used in this work was an exact replica of the spherical lens surface, and the resulting form of the etched micro-lens is investigated here.

The surfaces were profiled using a white light interferometer (Zygo Corporation). The measured surface, presented in Figure 3a, showed good overall form agreement with the nominal inscribed form. Deviations from the nominal form are highlighted in Fig 3b and c which show the lens profile after removal of a spherical fit with 0.975 mm radius.

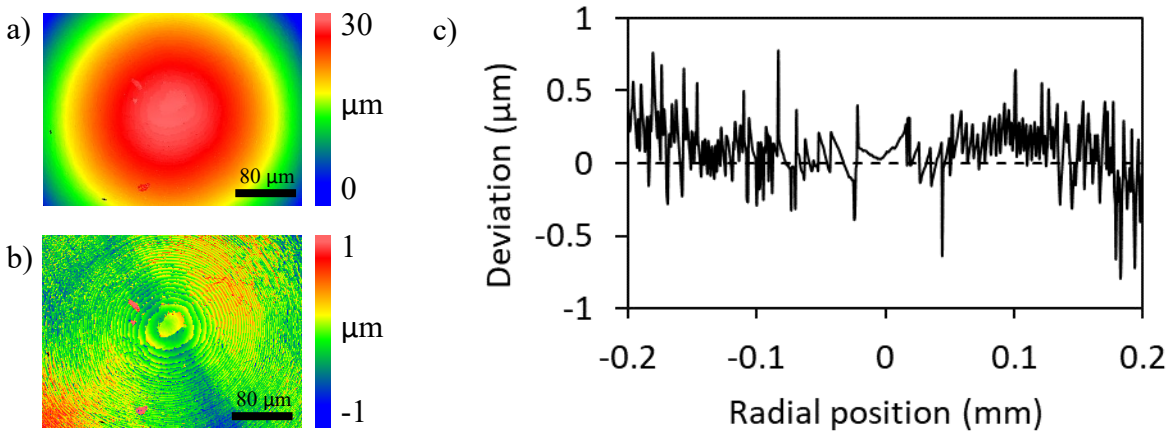

Figure 3: a) Microlens surface profile measured by interferometry. b) The same profile with a spherical fit subtracted to reveal the deviation from the nominal form and the corresponding line profile, (c).

3.2 Roughness and texturing

In addition to surface form errors, one would expect the lens surface to exhibit roughness associated with wet chemical etching. A somewhat less expected surface artifact, which is clearly visible in Fig 3a and b, is a pattern of step-like concentric rings centered around the lens apex. Upon observation, one may assume that the rings are the result of a discretized translation of the substrate through the focus. However, the true origin of the concentric structure is in fact well documented within the field and is due to the formation of directional planes of alternating oxygen-rich and oxygen-deficient silica regions[18,19] within the laser focus. The planes, known as nanogratings, permit highly selective etching and are formed perpendicular to the laser polarization orientation as demonstrated by Hnatovsky et al in [20]. The fundamental processes that drive nanograting formation have been studied by several groups[21], but is beyond the scope of this work. However, it is noted that nanogratings form only when the incident pulses fall within a specified pulse energy and pulse duration window, known as Type II modification [22,23]. To investigate the effect of nanograting formation on the fabricated lens surface quality, additional microlenses were written with an increased pulse energy of 600 nJ, corresponding to Type III modification in which nanogratings collapse and micro voids form. It was found that when written type III modification, the microlens surface etched at a similar rate to when written with Type II modification. Figure 4b shows a micrograph of the Type III lens profile after etching. When compared with Figure 4a depicting Type II modification, it can be seen that the nanoplane impression on the lens surface has diminished, as expected.

To quantify the surface roughness of the microlenses written in these two regimes, an atomic force microscope (AFM) was used. The microlenses were sampled by the AFM at various points across the clear aperture with each scan covering a 63 × 63 µm area. A polynomial fit was performed on each measurement to account for the lens curvature, and deviations from this fit were used to determine both average and peak-to-peak roughness. The lens inscribed with 200 nJ pulses had an arithmetic mean areal roughness of 47.6 nm and a pk-pk roughness of 447.6 nm. The lens inscribed with 600 nJ pulses had an arithmetic mean areal roughness of 35.4 nm and a peak-to-peak roughness of 320.5 nm. Although the Type III lens lacked textural structure compared to the Type II lens, as seen in Figure 4c and d, both lenses exhibited significant pk-pk roughness on the order of the wavelength of visible light. This level of roughness would be expected to generate significant levels of optical scattering. Therefore, a post-process flame polishing technique was explored.

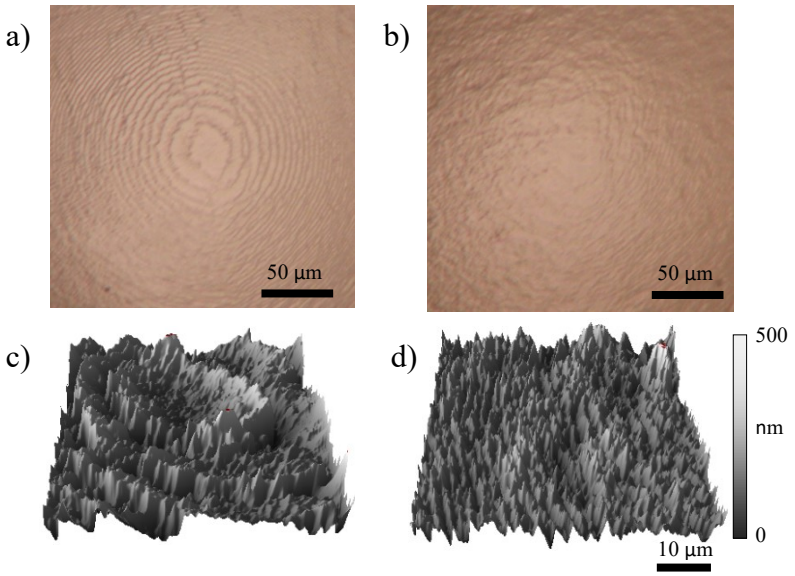

Figure 4: Micrographs of the lens surfaces after fabrication using (a) 200 nJ pulses and (b) 600 nJ pulses and their corresponding AFM scans with nominal form removed to highlight roughness and texturing (c) and (d). The concentric rings that appear in (a) and (c) are explained by the formation of *nanogratings* which form perpendicular to the laser polarization during femtosecond laser writing under certain irradiation conditions

3.3 Flame polishing

Flame brushing was explored to decrease surface roughness of the microlens after etching. Flame brushing was performed using a miniature oxyhydrogen torch (AQUAFLAME SYSTEMS MODEL 500) generating a 3 mm long 1850˚ C flame through a 21-gauge nozzle. Microlenses were translated through the tip of the flame at various translation speeds to control the effect of thermal melting and reflow. When controlled correctly, the flame melts only the high-frequency roughness peaks while the bulk material remains solid. While heating, surface tension draws the thin melt zone over the surface to smooth out the roughness without significantly modifying the nominal form of the lens. Both translation speed and the number of passes through the flame were investigated for optimum polishing parameters. We observed that after the first pass, subsequent passes had little and lessening effect on the surface roughness, and that an optimum speed existed where the overall form of the lens remained unchanged while the roughness was significantly reduced. The optimum speed for polishing the microlenses was approximately 2 mms^{-1}, but we note that the optimum speed is likely to vary significantly for different surface forms. The form and roughness were measured using an interferometer and AFM respectively. Example surface measurements are presented in Figure 5. We found that the arithmetic areal roughness could be repeatably reduced from around 50 nm post etch, to 2-4 nm post polish. Deviation from the nominal form, presented in Figure 5c and d, was comparable in range to that of the pre-polished lens presented in Figure 3c.

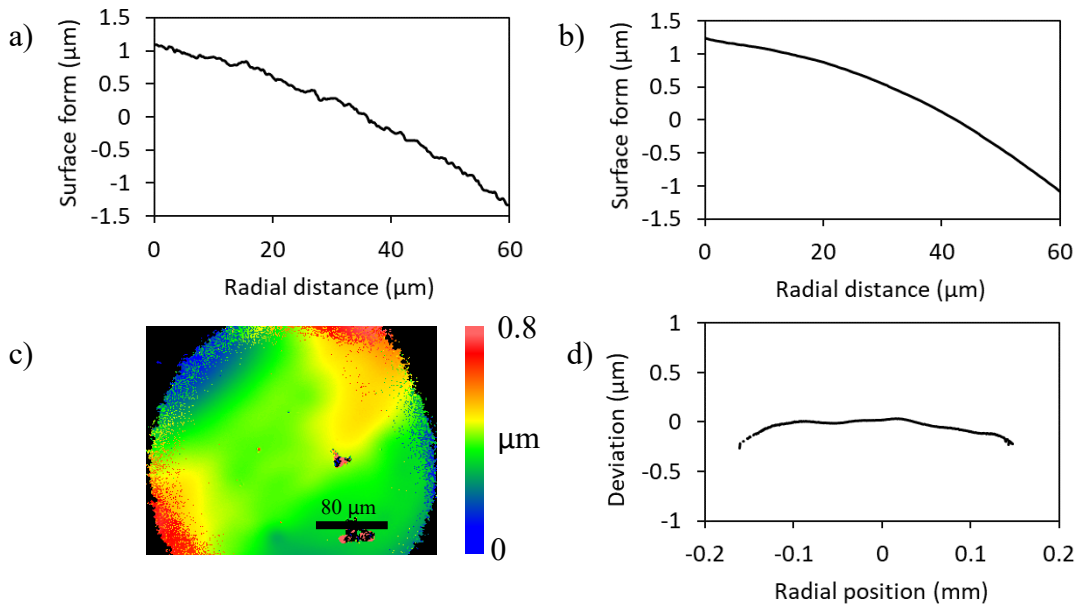

Figure 5: AFM scans of a microlens surface before (a) and after (b) flame polishing. The roughness was significantly reduced after flame brushing, while the deviation from the nominal form remained low as shown in (c) and (d).

3.4 Passive alignment

Fiber coupling was assisted by a passive alignment slot written into the monolithic micro-optic. To test the alignment precision and repeatability of the alignment slot, stripped single-mode fiber (SM600, Thorlabs) was inserted in and out of the slot repeatedly and the lateral core position mapped each time. A histogram of the lateral core positions for 100 insertions is presented in Figure 6a. The variance in lateral fiber positioning was determined to be 0.83 µm and 0.52 µm in the horizontal and vertical axes respectively to ± 2 standard deviations. The difference in precision along the two orthogonal axes was due to a slight ellipticity in the alignment slot cross section.

For multimode fiber light coupling applications, the fiber core typically needs to be aligned with the microlens optical axis to a precision of less than a few micrometers, achieved here using the alignment slot. The final step in constructing the coupler was to bond the fiber inside the slot. This was done using an ultraviolet cured optical adhesive (NOA61 Norland). The adhesive was applied to the end of a multimode 50 µm core diameter fiber with 0.22 NA (FG050LGA, Thorlabs), and the fiber inserted into the slot. The far-field light distribution was observed during bonding to ensure no air-bubbles were present at the end of the fiber and the adhesive was set under UV light for five minutes. A photograph of the resulting lens coupler is presented in Figure 6b.

3.5 Optical performance

Once assembled, the lens couplers were optically characterized in terms of their transmission, far field collimation and fiber coupling efficiency. To test the transmission, 633 nm He-Ne laser light was sent down the fiber and the light power in the far field after transmission through the micro-optic was measured. The average throughput of five unpolished lenses was found to be 95.2 ± 1.8%, which rose to 98.0 ± 2.0% for polished lenses. The divergence of the beam launched from the fiber upon transmission through the lens was also determined by measuring the extents of the far field light distribution at a series of distances along the optical axis. The far-field beam had a divergence of 34.4 mrad – higher but comparable to the theoretical value of 21.8 mrad obtained by a ray trace simulation of an ideal system. Finally, the fiber coupling efficiency of the lens coupler was measured by directing collimated light at the lens surface and measuring the power transmitted through the optical fiber. We found that 76.2% of light which filled the circular clear aperture of the lens was coupled into the optical fiber.

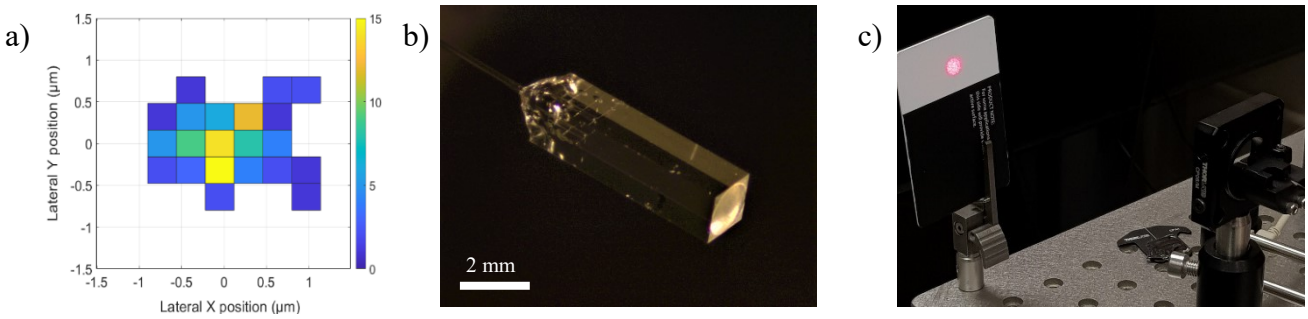

Figure 6: (a) A histogram of the variance in lateral position of the optical fiber passively constrained by the alignment slot. (b) A micrograph of the assembled lens coupler and the far-field output from a multimode fiber at 150 mm, (c).

4. CONCLUSION AND OUTLOOK

We have demonstrated a laser-based fabrication method for micro-optic systems in fused silica glass, with advantages over current manufacturing methods including micron-level feature size and precision, integrated passive alignment capabilities and freeform surface compatibility. The method is inexpensive and well suited to rapid prototyping but also has scaling-up potential. For demonstration, we fabricated a micro-optic lens coupler with an integrated alignment slot for passive optical fiber alignment to the lens. Flame brushing was used to reduce surface roughness by over an order of magnitude to levels repeatedly < 5 nm and < 10 nm for arithmetic and peak-peak roughness respectively. These values are comparable with commercially available lenses of similar form. The overall form of the lens showed close agreement with the specified design in terms of radius, but did show significant surface form error. We suspect this is due to an anisotropic laser-induced modification over the lens surface and subsequent etch. To improve the lens form, several factors may be investigated including writing in a longitudinal geometry, optimizing the tool path to consider the asymmetric focal region, varying the polarization orientation dynamically during inscription, or applying beam shaping techniques to the focus. Nonetheless, the microlens performed well, with an average multimode fiber coupling efficiency of 76.2%.

Recently, attention has turned to using advanced techniques to ready ULAE for industry level manufacturing and indeed several commercial ventures specializing in ultrafast-laser-based fabrication in glass now exist. Key developments in ULAE research include the use of elongated *Bessel* beams which allow orders of magnitude faster material processing rates to reduce inscription time significantly[24]. Wavefront shaping and spatio-temporal focusing have also been explored as ways to increase the selectivity of the etching process[15,25,26], reduce writing aberrations and increase substrate size constraints – all of which are crucial steps for elevating ULAE towards industrial scale manufacturing.

5. REFERENCES

[1] Cirasuolo, M. and Consortium, the M., "MOONS: The New Multi-Object Spectrograph for the VLT," arXiv [astro-ph.IM] **180**(arXiv:2009.00628), 10–17 (2020).

[2] Montgomery, D., Atkinson, D., Beard, S., Cochrane, W., Drass, H., Guinouard, I., Lee, D., Taylor, W., Rees, P. and Watson, S., "Development of the fibre positioning unit of MOONS," Ground-based Airborne Instrum. Astron. VI **9908**, SPIE (2016).

[3] Guinouard, I., Horville, D., Lee, D., Watson, S., Reesb, P. and Flores, H., "Assemblies of the microlenses on the front-end fibres of MOONS," Proc. SPIE 11451 - 247 (2020).

[4] Thomson, R. R., Birks, T. A., Leon-Saval, S. G., Kar, A. K. and Bland-Hawthorn, J., "Ultrafast laser inscription of an integrated photonic lantern," Opt. Express **19**(6), 5698–5705 (2011).

[5] MacLachlan, D. G., Thomson, R. R., Cunningham, C. R. and Lee, D., "Mid-Infrared Volume Phase Gratings Manufactured using Ultrafast Laser Inscription," Opt. Mater. Express **3**(10), 1616 (2013).

[6] Mikutis, M., Kudrius, T., Šlekys, G., Paipulas, D. and Juodkazis, S., "High 90% efficiency Bragg gratings formed in fused silica by femtosecond Gauss-Bessel laser beams," Opt. Mater. Express **3**(11), 1862 (2013).

[7] Chen, W.-J., Eaton, S. M., Zhang, H. and Herman, P. R., "Broadband directional couplers fabricated in bulk glass with high repetition rate femtosecond laser pulses," Opt. Express **16**(15), 11470 (2008).

[8] Ross, C. A., MacLachlan, D. G., Smith, B. J. E., Beck, R. J., Shephard, J. D., Weston, N. and Thomson, R. R., "A Miniature Fibre-Optic Raman Probe Fabricated by Ultrafast Laser-Assisted Etching," Micromachines **11**(2), 185 (2020).

[9] Sugioka, K. and Cheng, Y., "Femtosecond laser processing for optofluidic fabrication," Lab Chip **12**(19), 3576 (2012).
[10] Sima, F., Sugioka, K., Vázquez, R. M., Osellame, R., Kelemen, L. and Ormos, P., "Three-dimensional femtosecond laser processing for lab-on-a-chip applications," Nanophotonics **7**(3), 613–634 (2018).
[11] Guinouard, I., Avila, G., Lee, D., Amans, J.-P., Rees, P., Taylor, W. and Oliva, E., "Design, development, and performance of the fibres of MOONS," Adv. Opt. Mech. Technol. Telesc. Instrum. II **9912**, R. Navarro and J. H. Burge, Eds., 99125G, SPIE (2016).
[12] Hnatovsky, C., Taylor, R. S., Simova, E., Bhardwaj, V. R., Rayner, D. M. and Corkum, P. B., "Polarization-selective etching in femtosecond laser-assisted microfluidic channel fabrication in fused silica," Opt. Lett. **30**(14), 1867–1869 (2005).
[13] Richter, S., Plech, A., Steinert, M., Heinrich, M., Döring, S., Zimmermann, F., Peschel, U., Kley, E. B., Tünnermann, A. and Nolte, S., "On the fundamental structure of femtosecond laser-induced nanogratings," Laser Photon. Rev. **6**(6), 787–792 (2012).
[14] Shimotsuma, Y., Kazansky, P. G., Qiu, J. R. and Hirao, K., "Self-organized nanogratings in glass irradiated by ultrashort light pulses," Phys. Rev. Lett. **91**(24), 4 (2003).
[15] Huang, L., Salter, P. S., Payne, F. and Booth, M. J., "Aberration correction for direct laser written waveguides in a transverse geometry," Opt. Express **24**(10), 10565–10574 (2016).
[16] Oliva, E., Delabre, B., Tozzi, A., Ferruzzi, D., Lee, D., Parry, I. and Rees, P., "Toward the final optical design MOONS, the Multi-Object Optical and Near infrared Spectrometer for the VLT," Ground-based Airborne Instrum. Astron. VI **9908**, C. J. Evans, L. Simard, and H. Takami, Eds., 99087R, SPIE (2016).
[17] Ross, C. A., MacLachlan, D. G., Choudhury, D. and Thomson, R. R., "Optimisation of ultrafast laser assisted etching in fused silica," Opt. Express **26**(19), 24343 (2018).
[18] Richter, S., Heinrich, M., Döring, S., Tünnermann, A., Nolte, S. and Peschel, U., "Nanogratings in fused silica: Formation, control, and applications," J. Laser Appl. **24**(4), 042008 (2012).
[19] Drevinskas, R., Gecevičius, M., Beresna, M., Bellouard, Y. and Kazansky, P. G., "Tailored surface birefringence by femtosecond laser assisted wet etching," Opt. Express **23**(2), 1428 (2015).
[20] Hnatovsky, C., Taylor, R. S., Simova, E., Rajeev, P. P., Rayner, D. M., Bhardwaj, V. R. and Corkum, P. B., "Fabrication of microchannels in glass using focused femtosecond laser radiation and selective chemical etching," Appl. Phys. a-Materials Sci. Process. **84**(1–2), 47–61 (2006).
[21] Zhang, B., Liu, X. and Qiu, J., "Single femtosecond laser beam induced nanogratings in transparent media - Mechanisms and applications," J. Mater. **5**(1), 1–14 (2019).
[22] Hnatovsky, C., Taylor, R. S., Rajeev, P. P., Simova, E., Bhardwaj, V. R., Rayner, D. M. and Corkum, P. B., "Pulse duration dependence of femtosecond-laser-fabricated nanogratings in fused silica," Appl. Phys. Lett. **87**(1), 014104 (2005).
[23] Richter, S., Heinrich, M., Doring, S., Tunnermann, A. and Nolte, S., "Formation of femtosecond laser-induced nanogratings at high repetition rates," Appl. Phys. a-Materials Sci. Process. **104**(2), 503–507 (2011).
[24] Bhuyan, M. K., Courvoisier, F., Lacourt, P.-A., Jacquot, M., Furfaro, L., Withford, M. J. and Dudley, J. M., "High aspect ratio taper-free microchannel fabrication using femtosecond Bessel beams," Opt. Express **18**(2), 566 (2010).
[25] Sun, B., Salter, P. S. and Booth, M. J., "Pulse front adaptive optics: a new method for control of ultrashort laser pulses," Opt. Express **23**(15), 19348 (2015).
[26] Wang, Z., Jiang, L., Li, X., Wang, A., Yao, Z., Zhang, K. and Lu, Y., "High-throughput microchannel fabrication in fused silica by temporally shaped femtosecond laser Bessel-beam-assisted chemical etching," Opt. Lett. **43**(1), 98 (2018).